A Low Aberration Negative Liquid Crystal Lens

Tzu-Yu Tai[1], Wei-Wei Chen[1], Jui-Wen Pan[2], Shie-Chang Jeng[3,*]

* e-mail: scjeng@faculty.nctu.edu.tw, scjeng@nycu.edu.tw
[1]Institute of Lighting and Energy Photonics National Yang Ming Chiao Tung University, Taiwan,
[2]Institute of Photonic System National Yang Ming Chiao Tung University, Taiwan,
[3]Institute of Imaging and Biomedical Photonic National Yang Ming Chiao Tung University, Taiwan.
Keywords: Hole-patterned electrodes, Liquid crystal lens, Low aberration

ABSTRACT

A hole-patterned electrodes (HPE) liquid crystal (LC) lens is developed by using a homeotropically-aligned LC cell. Low aberration is obtained because the LC directors are well aligned along with the axially symmetrical electrical field. The optical-path difference of the HPE LC lenses is less than λ/4 in all directions.

1 Introduction

HPE LC lenses have been intensively studied for photonic applications due to their ease of fabrication and simplicity of the device structure [1]. However, the conventional HPE LC lens has several drawbacks due to the pretilt angle and the nonsymmetric structures between the applied electric filed and LC alignment direction: such as disclination [2] and aberration [3-5]. Various LC lenses based on the HPE structure have been developed to solve these problems [6]. Reduction of aberration can be solved by using stacked LC structures with opposite pretilt angles [7] or by the splitting of the HPE [8]. The disclination lines can be prevented by the application of LC cells with high pretilt angles [9].

In this paper, we report on the realization of HPE LC lens with the properties of a controllable negative diopter, that is easy to fabricate, and most importantly, has low aberration, developed using a homeotropically-aligned LC cell by photoalignment technique [10]. The low aberration is obtained because both the LC directors and the electric field are axially symmetrical. The aberration of our proposed LC lens is systematically measured and studied using a wavefront sensor and the Zernike polynomial, respectively.

2 Experiment

A schematic representation of the operating principles of the single-layer HPE LC lens with the LC material (Δε= -2.8, Δn=0.096, no=1.483, DIC Corp.) is shown in Fig. 1. The indium tin oxide (ITO) film is applied on the inner surface of the lower substrate for acting as one electrode. The outer surface of upper substrate is covered by an aluminum film with a 4.5 mm diameter hole to act as a second electrode. The cell gap of the LC layer is controlled by the 75 μm mylar films. The inner surfaces of the substrates are further prepared by spin coating with photo-crosslinking polyimide (PI) materials [10]. A linear polarization ultraviolet light source (EXECURE 4000 with a Glan Taylor polarizing prism, HOYA) is incident on the PI alignment film with an angle of 40° relative to the normal (26.5 mW/cm^2 with an 11 seconds exposure time). Four layers of the HPE LC lenses are assembled to obtain a large optical power for LC lens applications. The diopter of the HPE LC lens can range in value from zero to a negative value by the application of different driving voltages.

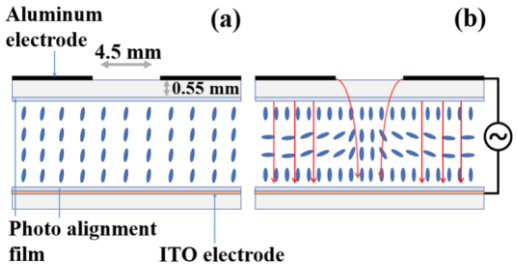

Fig.1. A schematic representation of the working principles of the HPE LC lens: (a) without a driving voltage (b) for a negative lens at 1kHz.

3 Results and Discussion

From the interference fringes shown in Fig. 2, the focal length f of the proposed LC lens can be calculated by [11]:

$$f = \frac{r^2}{2N\lambda}$$

where r is the radius of the LC lens aperture, λ is the wavelength of the light, and N is the number of the interference fringe.

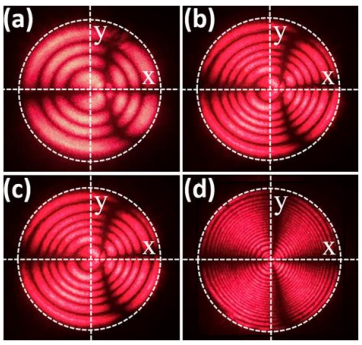

Fig. 2. Interference patterns with different LC cell gaps: (a) 25μm (b) 50μm (c) 75μm (d) 125μm.

Fig. 3 shows the diopter of the HPE LC lens as a function of the applied voltage (1 kHz square wave). The absolute value of negative diopter single-layer and four-layer HPE LC lenses increases with the applied voltage from 0 to ~1.2 D and 0 to ~5.0 D, respectively. The advantage of the axially symmetric distribution of the LC directors is that it is not necessary to consider the orientation of the HPE LC lens direction when stacking multi-layer structures.

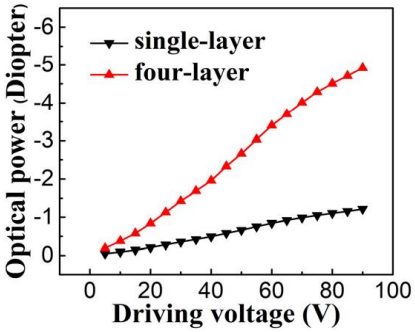

Fig. 3. Diopter of the HPE LC lenses as a function of the applied voltage.

Fig. 4 illustrates the phase profile across the aperture of the as-prepared LC lens calculated from the interference patterns, where the ideal quadratic curves are indicated by solid lines. The phase retardation profile shown in Fig. 4 is commonly applied to analyze the quality of an LC lens. However, the results shown in Fig. 4 do not directly reflect quality of the HPE LC lens for imaging applications, so the Zernike polynomial is subsequently applied to systematically analyze the aberrations of the optical wavefront of the as-prepared HPE LC lens.

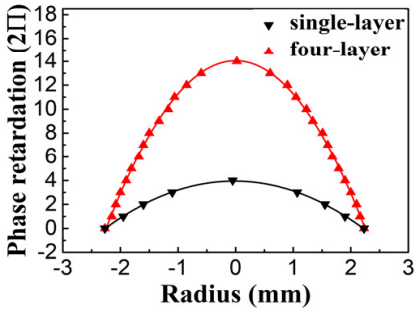

Fig. 4. Phase retardation of single-layer and four-layer HPE LC lenses operated at 60 V.

Fig. 5 shows the Zernike coefficient of the single-layer and four-layer HPE LC lenses for different optical powers. The aberration increases only slightly with the optical power for both the single-layer and four-layer HPE LC lenses. The Zernike coefficients of $C_{1,1}$ x-tilt, $C_{3,-1}$ y-coma, and $C_{3,1}$ x-coma are all less than -0.025λ for different optical powers due to the low aberration of our HPE LC lens. There is a slight increase in the $C_{1,-1}$ y-tilt and C4,0 spherical aberration to -0.027 λ and -0.034 λ, respectively, with the optical power for the four-layer HPE LC lenses. For a conventional HPE LC lens, the LC directors are aligned along the rubbing direction (for example, y-direction), therefore the LC directors as seen in the cross-section are non-symmetric along the y-direction due to the pretilt angle [3]; it also exhibits a large coma aberration due to a strong twist deformation [12]. In our proposed scheme, the LC directors align with the electric field as well as with the axial symmetry, so the tilt and coma aberration are reduced to very small values in both the y-direction and the x-direction for both single-layer and four-layer HPE LC lenses.

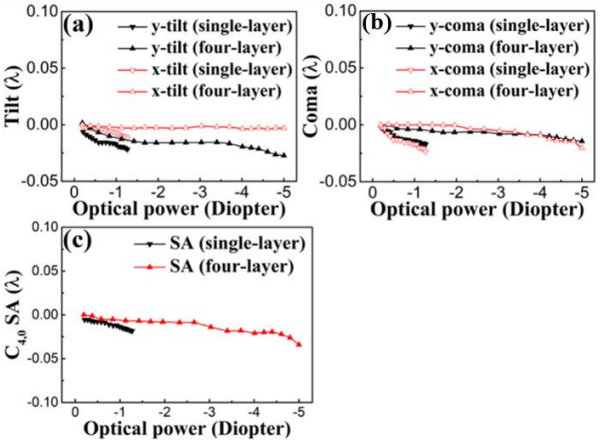

Fig. 5. Wavefront aberration for HPE LC lenses as a function of the diopter: (a) tilt of the HPE LC lens (b) coma of the HPE LC lens (c) SA of the HPE LC lens. SA: spherical aberration.

The OPD(ρ,θ)s of the HPE LC lenses are shown in Fig. 6. In order to estimate the aberration that can be tolerated in an imaging system, Rayleigh's quarter wavelength rule is often applied as a useful criterion [13]. The performance for imaging applications must follow the Rayleigh quarter wavelength rule, so the absolute value of the OPD(ρ,θ)s should be below λ/4 (dashed line). Only the aberration at ρ=1 and at the θ with the maximum sinusoidal value is considered because the most severe wavefront aberration happens near the electrode. As can be seen in Fig. 6, the OPD(ρ,θ)s of the HPE LC lenses are less than λ/4 in both the y-direction and the x-direction for each diopter, for both of the single-layer and the four-layer structure. From the results illustrated in Fig. 6, we can conclude that the performance of the as-prepared HPE LC lenses is good enough for imaging applications.

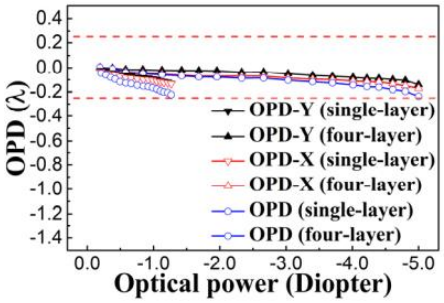

Fig. 6. OPD of the HPE LC lenses as a function of the diopter.

4 Conclusions

In this Letter, we demonstrate a four-layer HPE LC lens with the adjustable optical power from 0 to -5.0 D by the application of different voltages. The tilt and coma aberration for the x-axis and y-axis are at least 10 times smaller than those of the conventional HPE LC lens [12]. The OPD(ρ,θ)s of the HPE LC lenses are less than λ/4 in both the y-direction and the x-direction.

Acknowledgments

Ministry of Science and Technology, Taiwan (MOST109-2622-E-009-012-CC2, MOST 107-2112-M-009-007-MY3 and MOST 110-2112-M-A49-030).

References

[1] J. F. Algorri, D. C. Zografopoulos, V. Urruchi, and J. M. Sanchez-Pena, Crystals 9, 272 (2019).

[2] M. Ye, B. Wang, and S. Sato, Appl. Phys. 42, 5086 (2003).

[3] T. Scharf, P. Kipfer, M. Bouvier, and J. Grupp, Appl. Phys. 39, 6629 (2000).

[4] T. Takahashi, M. Ye, and S. Sato, Appl. Phys. 46, 2926 (2007).

[5] M. Ye, and S. Sato, Appl. Opt. 40, 6012 (2001).

[6] S. Sato, Opt. Rev. 6, 471 (1999).

[7] B. Wang, M. Ye, and S. Sato, Appl. Phys. 45, 7813 (2006).

[8] L. Begel, and T. Galstian, Appl. Opt. 57, 5072 (2018).

[9] T. Nose, S. Masuda, and S. Sato, Mol. Cryst. Liq. Cryst. 199, 27 (1991).

[10] V.G. Chigrinov, V.M. Kozenkov, H.S. Kwok, Photoalignment of liquid crystalline materials: physics and applications (Wiley, 2008).

[11] H. Ren, D. W. Fox, B. Wu, and S.-T. Wu, Opt. express, 15, 11328 (2007).

[12] J.J. Gao, J.W. Pan and S.C. Jeng, Opt. Lett. 45, 5077 (2020).

[13] W.J. Smith, Modern Optical Engineering (McGraw Hill, 2008).